Published in final edited form as:
*J Nucl Cardiol*. 2009 ; 16(2): 201–211. doi:10.1007/s12350-008-9019-z.

# Diagnostic performance of fusion of myocardial perfusion imaging (MPI) and computed tomography coronary angiography

**Cesar A. Santana, MD**[a], **Ernest V. Garcia, PhD**[a], **Tracy L. Faber, PhD**[a], **Gopi K. R. Sirineni, MD**[a], **Fabio P. Esteves, MD**[a], **Rupan Sanyal, MD**[a], **Raghuveer Halkar, MD**[a], **Mario Ornelas, MD**[a], **Liudmila Verdes, MD**[a], **Stamatios Lerakis, MD**[b], **Julie J. Ramos, MD**[b], **Santiago Aguadé-Bruix, MD**[c], **Hugo Cuéllar, MD**[d], **Jaume Candell-Riera, MD**[e], and **Paolo Raggi, MD**[a,b]

[a]Department of Radiology, Emory University, Atlanta, GA

[b]Division of Cardiology, Emory University, Atlanta, GA

[c]Department of Nuclear Medicine, Vall d' Hebron University Hospital, Barcelona, Spain

[d]Department of Radiology, Vall d' Hebron University Hospital, Barcelona, Spain

[e]Department of Cardiology, Vall d' Hebron University Hospital, Barcelona, Spain

## Abstract

**Background—**We evaluated the incremental diagnostic value of fusion images of coronary computed tomography angiography (CTA) and myocardial perfusion imaging (MPI) over MPI alone or MPI and CTA side-by-side to identify obstructive coronary artery disease (CAD > 50% stenosis) using invasive coronary angiography (ICA) as the gold standard.

**Methods—**50 subjects (36 men; 56 ± 11 years old) underwent rest-stress MPI and CTA within 12-26 days of each other. CTAs were performed with multi-detector CT-scanners (31 on 64-slice; and 19 on 16-slice). 37 patients underwent ICA while 13 subjects did not because of low (<5%) pre-test likelihood (LLK) of disease. Three blinded readers scored the images in sequential sessions using (1) MPI alone (2) MPI and CTA side-by-side, (3) fused CTA/MPI images.

**Results—**One or more critical stenoses during ICA were found in 28 patients and non-critical stenoses were found in 9 patients. MPI, side-by-side MPI-CTA, and fused CTA/MPI showed the same normalcy rate (NR:13/13) in LLK subjects. The fusion technique performed better than MPI and MPI and CTA side-by-side for the presence of CAD in any vessel (overall area under the curve (AUC) for fused images: 0.89; $P = .005$ vs MPI, $P = .04$ vs side-by-side MPI-CTA) and for localization of CAD to the left anterior descending coronary artery (AUC: 0.82, $P < .001$ vs MPI; $P = .007$ vs side-by-side MPI-CTA). There was a non-significant trend for better detection of multi-vessel disease with fusion.

**Conclusions—**Using ICA as the gold standard, fusion imaging provided incremental diagnostic information compared to MPI alone or side-by-side MPI-CTA for the diagnosis of obstructive CAD and for localization of CAD to the left anterior descending coronary artery.

### Keywords

Myocardial perfusion imaging; SPECT; PET imaging; computed tomography (CT); coronary artery disease; diagnostic and prognostic application



Reprint requests: Paolo Raggi, Department of Radiology, Emory University, 1365 Clifton Road NE, AT-504, Atlanta, GA 30322; praggi@emory.edu, raggip@gmail.com..

## INTRODUCTION

The gold standard for the visualization of the coronary arteries and detection of coronary artery stenoses is invasive coronary angiography (ICA). Often, the decision to revascularize a territory of the myocardium is based on the presence of an optical impression of luminal stenosis. However, the cost, risk, and invasive nature of coronary angiography render a reliable non-invasive method, with the ability to provide a better assessment of which vessel with obstruction needs intervention, very desirable. Approximately 40%-50% of the invasive coronary arteriograms performed in the United States each year do not demonstrate obstructive coronary artery disease (CAD)[1] and about half of the ICAs demonstrating CAD are followed by an interventional procedure.[1] Thus, in the interest of sparing health care resources and limit unnecessary invasive testing, a reliable non-invasive tool might be highly desirable.[2] Multi-detector CT coronary angiography (CTA) provides a safe, and non-invasive alternative to cardiac catheterization. Nevertheless, well-recognized limitations in the assessment of coronary stenoses with CTA are related to motion artifacts, coronary arterial calcification, coronary stenting and the clear assessment of luminal stenosis in distal coronary arteries.

Myocardial perfusion imaging (MPI) offers a powerful approach to cost effective management of CAD, although it too suffers from some limitations. For example, in patients with diaphragmatic or breast attenuation, photopenic myocardial regions can be misinterpreted for hypoperfusion. In such cases, CTA with its high negative predictive value could obviate the need for ICA. Thus, MPI and CTA are potentially complementary techniques, since MPI assesses physiology and CTA morphology and their inherent technical limitations are quite different.

In current clinical practice, a physician subjectively performs the integration of anatomic and physiologic information from angiograms and MPI. The two image sets are viewed independently, and integration of the information is performed mentally. However, in some cases the location of a stenosis with respect to the left ventricular epicardial surface can only be judged with considerable approximation. The existence of more than one stenosed artery exacerbates this problem, especially if the degree of stenosis is unclear since such stenoses may or may not cause perfusion abnormalities. Additionally, the use of quantitative analysis tools in MPI is not as popular as the visual interpretation of the tomographic images. We have preliminarily observed that when the coronary tree extracted from CTA is super-imposed using image fusion onto the left ventricular myocardial perfusion map, true positive critical lesions from CTA are aligned on the corresponding hypoperfused vascular territories identified by MPI. This alignment (or lack of alignment in normal regions) is very helpful in the image interpretation process particularly when the information from CTA or MPI is degraded for technical reasons. The aim of the present study was to evaluate if the fusion of CTA and MPI images has incremental diagnostic value over MPI alone or MPI and CTA read side-by-side for the identification of obstructive CAD using ICA as the gold standard. We were also interested to verify whether image fusion may help exclude patients with non-critical lesions from undergoing unnecessary ICA.

## MATERIALS AND METHODS

### Study Population

Fifty-five patients were consented for this study; however 5 were excluded because either the MPI (2 patients) or the CTA (3 patients) studies were not acquired. The remaining 50 consecutive subjects (36 (72%) men, mean age: 56 ± 11 years) who underwent stress myocardial perfusion imaging and CTA within 12 ± 26 days of each other were included in this study. Thirteen of the 50 subjects were normal volunteers. These 13 volunteers had a

low pre-test likelihood of CAD (LLK) defined as having lower than 5% probability of CAD based on sequential Bayesian analysis of age, gender, and symptom classification.[3] The remaining 37 patients underwent MPI, CTA, and ICA within 90 days (range 1-89) without intervening relevant therapeutic or clinical changes. Nine of the 37 patients who underwent ICA were found to have non-critical lesions and were used to help establish the specificity of the various interpretations. A written informed consent was obtained from each patient in accordance with the guidelines on human investigations as established by the internal review board of Emory University, Atlanta, GA, USA, and Vall d' Hebron University Hospital, Barcelona, Spain.

## Myocardial Perfusion Imaging

Thirty-four of the 50 patients underwent SPECT MPI of which 19 were performed in Vall d' Hebron University Hospital (Barcelona, Spain). These 19 patients underwent exercise-stress/rest Tc-99m Tetrofosmin MPI. Fifteen SPECT studies were acquired at Emory University Hospital (Atlanta, GA) and these patients underwent exercise-stress/rest Tc-99m Sestamibi MPI. Finally, 16 patients underwent adenosine stress Rb-82 PET at Emory University Hospital. Only 1 of the 13 LLK subjects underwent imaging at Vall d' Hebron University Hospital, Barcelona, Spain, with SPECT and 16-slice CTA.

## SPECT Protocol

All scans were performed using either a dual detector Millennium MG camera (GE, Healthcare, USA) at Emory University or a Siemens E-CAM (Erlangen, Germany) dual-head camera at Vall d'Hebron University Hospital. Conventional SPECT projections were obtained utilizing a previously described simultaneous emission/transmission acquisition method that uses a scanning gadolinium-153 line source as the transmission source.[4] Briefly, patients were asked to stop taking nitrates for 6 hours, calcium-channel blockers for 24 hours, and ß-blockers for 48 hours before the cardiac SPECT scan. The images were corrected for attenuation, scatter, and resolution effects. The Tc-99m (Sestamibi or Tetrofosmin) doses, adjusted for body weight, were 333-555MBq (9-15 mCi) for rest and 814-1665MBq (22-45mCi) for stress. A stress injection of the Tc-99m perfusion tracer was administered during peak exercise of a Bruce treadmill protocol.

The images were acquired with a low-energy high-resolution collimator, by use of a 180° non-circular orbit from 45° right anterior oblique to left posterior oblique, with a 64 × 64 matrix (pixel size of approximately 0.64 cm) for the emission images and a 128 × 128 matrix (pixel size of 0.32 cm) for the transmission images. The data were collected in three individual photopeaks: (1) emission, 140 keV ± 10%; (2) transmission, 100 keV ± 10%; and (3) scatter, 118 keV ± 6%. A total of 64 simultaneous emission, transmission, and scatter projections were obtained (usually 25-30 seconds per projection).

Each of the projection images were corrected for non-uniformity with a flood source image containing 30 million counts, and the mechanical center of rotation was determined to align the projection data with respect to the reconstruction matrix. The projection images from the rest and stress studies were then automatically corrected for radioactive decay occurring during acquisition. The emission images were reconstructed with attenuation correction. Myocardial perfusion transverse images were reconstructed by first pre-filtering the emission projections with a fifth-order 0.66 Nyquist Butterworth filter followed by reconstructing via an iterative maximum likelihood expectation maximization algorithm. Attenuation maps were reconstructed by use of a previously described algorithm that uses a Bayesian prior approach with Butterworth filter pre-processing at 0.43 critical frequency and an order of 5.0.[5] The scatter distribution obtained from the scatter window was used to correct both the scatter from the patient onto the photopeak window and the scatter from the

patient onto the transmission energy window. All attenuation maps automatically underwent quality control for adequate counts, field uniformity, and truncation.[6]

## PET Protocol

All scans were acquired using a GE Discovery ST PET/ CT scanner (GE Healthcare, USA), comprising a full 6.3 × 6.3 × 30 $mm^3$ bismuth germanate (BGO) block detector ring of 157 mm field-of-view operating in 2D mode. The CT employs a 16-slice detector array with a tube current range of 10-440 mA, peak kilovoltage range of 80 to 140 kVp, and maximum gantry rotation speed of 3 Hz. The scanner is equipped with a cardiac gating input, which receives a forward R-wave trigger pulse supplied by an ECG. The images were acquired following conventional methodology. Briefly, patients were asked to stop taking nitrates for 6 hours, calcium-channel blockers for 24 hours, and ß-blockers for 48 hours before the cardiac PET/CT scan and were instructed not to consume caffeine-containing products for 24 hours before the test.

The images were acquired as follows: a scout CT was done to check the patient position. Next, a slow CT attenuation scan was performed with the lowest pitch (0.562:1) allowed by the scanner, covering the chest cavity in 16 seconds while patients maintained a shallow breathing. Then a 1480-2220MBq (40-60 mCi) dose of Rb-82 was injected and a 7-minute dynamic rest 2D emission scan, followed by a 7-minute rest gated scan, was acquired. Pharmacologic stress was then started using adenosine (140 μg/kg/min × 6 minutes). A 1480-2220MBq (40-60 mCi) dose of Rb-82 was injected at the end of the second minute of adenosine infusion followed by a 7-minute dynamic stress 2D emission scan.[7]

Emission data were corrected for attenuation, scatter, and random events and reconstructed using the manufacturer supplied ordered-subsets estimation maximization (OSEM) algorithm (2 iterations, 28 subsets) with a Butterworth post-filter of cut-off frequency 0.45 and power 10. The studies were analyzed by summing all frames after the left ventricular cavity counts dropped to half of the cardiac tissue concentration. The magnitude of misalignment was assessed using the ImagenPro PET QC program (Cardiovascular Imaging Technologies, Kansas City, KS). Briefly, the misalignment was determined by visual inspection of the superimposed emission and transmission images. When misalignment was detected, the MPI images were manually realigned within the pericardial sac with careful avoidance of intersecting the lungs. Manual realignment of the transmission image was required in 30% of patients to ensure proper registration prior to image reconstruction.[6]

## Computed Tomography Coronary Angiography

Nineteen of the 50 CTA scans were performed in Vall d' Hebron Hospital (Barcelona, Spain) using the Siemens Sensation 16-slices multi-detector CT scanners (Erlangen, Germany). Thirty-one were acquired at Emory University Hospital (Atlanta, GA) using either a GE LightSpeed VCT 64-slice (GE Healthcare, USA) or a Siemens Sensation 64-slice CT scanner (Erlangen, Germany). Routine initial screening including vital signs in accordance with standard hospital and department of radiology policies were performed. ECG leads were placed on the chest and/or arms of the patient to gate the images. With the patient in a supine position a scout scan was performed to locate the borders of the heart to minimize the field of view. Once this was accomplished, an iodine bolus tracking method was utilized to determine the scan delay time. Estimation of scan delay time was used to optimize the visualization of the coronary arteries, by correctly timing the scan acquisition in relation to the contrast bolus. For this purpose, a small dose of iodinated contrast (20 cc of Omnipaque 350, GE Healthcare, USA) was injected through an IV access in the ante-cubital fossa and serial tomographic scans were acquired at the level of the bronchial carina, until peak enhancement was noted in the ascending aorta. The scanner software was used to

calculate the time to peak aortic enhancement. Scan delay time was calculated as peak aortic enhancement + 5 seconds. A dose of sublingual nitroglycerin was administered and a bolus of 100-120 cc of iodinated contrast (Omnipaque 350, GE Healthcare, USA) was injected at the rate of 5 cc/second followed by a saline chase of 30 cc at the rate of 5 cc/second. Scan acquisition was initiated after the scan delay time using routine parameters (120 KVp, 600-800 effective mAs, pitch 0.2 with helical acquisition, scan direction-craniocaudal, 16 × 0.75 $mm^2$ or 64 × 0.6 $mm^2$ detector configuration, and 0.33-0.40 second gantry rotation time for the 16- and 64-slice CT scanners, respectively). The saline chaser was used to flush out contrast from the superior vena cava and the right heart to reduce streak artifacts that may impede visualization of the right coronary artery.

Oral and occasionally intravenous beta-blockers were administered as needed prior to CTA to reduce the heart rate and keep it in the optimal range of 60 to 65 bpm. With this provision, the average heart rate at the time of CT coronary angiography was 61 ± 7 beats per minute.

Frequent monitoring of the patient in accordance with hospital guidelines was performed. Images were reconstructed using retrospective ECG gating at a phase of the R-R interval that allowed a relative motion-free visualization of the three main coronary arteries. This phase varied from case to case and usually ranged from 50% to 70% of R-R interval. The slice thickness and interslice distance of the reconstructed images were 0.75 mm and 0.5 mm, respectively. The images were processed into several different views, including standard axial, coronal, sagittal images along with maximum intensity projections, multi-planar reconstructions, curved multi-planar reformations, and volume rendering. Coronary vessels were identified and standard nomenclature for naming and numbering of the coronary arteries was used in accordance with ACC/AHA guidelines.[8] The CTAs were interpreted by two independent physicians who visually graded the severity of stenosis as mild <30% stenosis, moderate 30-70%, and severe >70%. The readers were also asked to grade the scans for quality on a scale of poor to excellent. The majority of scans were of good to excellent quality. However, the quality was poor to acceptable in 12% of the left coronary tree renderings due to the presence of coronary calcification and 34% of the right coronary tree renderings mostly due to motion artifact.

## Image Fusion

CTA scans were processed using the CardIQ program module in Advantage Windows Ver4.2 (GE Healthcare, USA) to detect and extract all visible branches of the main coronary arteries. The information of the extracted coronary arteries was stored in a Dicom file on the workstation and later transferred to the workstation handling the fusion process. Next, MPI images and the coronary arteries detected from CardIQ were processed using the HeartFusion program (Emory Cardiac Toolbox (ECTb), Syntermed, Atlanta, GA). Using the HeartFusion program, MPI transaxial slices were reformatted into short axis sections. Then, coronary artery points were transformed into transaxial MPI space, using the “frame of reference” point in the Dicom header and scaled based on pixel sizes. Next, standard perfusion quantification was performed and 3D LV epicardial surface was constructed. Coronary artery points were translated and rotated using the parameters from the short axis reorientation, so that they matched the reoriented MPI. Alignment was further refined by translating the proximal LAD to the basal anterior interventricular groove, and the PDA to the basal inferior interventricular groove. Finally, the arteries were warped onto (i.e. distorted and morphed to) the LV epicardial surface as described before.[9]

## Invasive Coronary Angiography

Coronary angiography was performed following standard percutaneous techniques. Two experienced angiographers interpreted all invasive studies assessing severity of stenosis

visually and reported the results by consensus. The criterion for a significant stenosis was set at ≥50% obstruction in at least one major coronary artery. For comparison with the perfusion study, left main coronary lesions were recorded as left anterior descending coronary artery (LAD) and left circumflex coronary artery (LCX) disease. Diagonal lesions were considered as part of the LAD, and obtuse marginal artery lesions were considered part of the LCX territory. Lesions of the posterior descending branch were recorded as right coronary artery (RCA).

### Images Interpretation and Analysis

The ECTb was used as a platform for image processing and visualization. Three nuclear specialists (two nuclear medicine, one cardiologist) scored the 50 MPI studies using a five-point scale (1 = normal, 2 = probably normal, 3 = equivocal, 4 = probably abnormal, 5 = abnormal) in three subsequent reading sessions: (1) using MPI alone; (2) using MPI plus CTA side-by-side; and (3) using MPI, CTA and 3D fused images. The goal of the MPI interpretation was to identify hypoperfusion matching a specific vascular territory eventually found to be obstructed on the gold standard ICA. Image interpretation of MPI studies was performed using the same procedure used in our usual clinical practice. The diagnostician uses ECTb to view rotating planar projections, rest and stress tomographic slices, animated gated displays, functional parameters, rest/stress polar maps using database quantification to highlight both hypoperfused and reversible segments, and computer generated rest/stress 17 segment scores. The diagnostician then integrates all of the available information to score the nuclear scan under examination using the five-point scale described above. This same scale was used in the current study to determine whether the patient's images demonstrated the presence of CAD, and if so, to localize it to one or more of three major vascular territories (LAD, LCX, RCA). Scores three or greater were considered positive for disease when correlating with ICA. Since ICA cannot be used as a gold standard for detecting ischemia, only segments with reversible perfusion defects were used by the interpreter to increase the confidence of detecting CAD.

During session 2 and 3, the readers were allowed to review their previous interpretation and were allowed to reach a different interpretation for session 2 compared to session 1 and for session 3 as compared to sessions 1 or 2. At no time were the readers allowed to change their original interpretations based on information newly acquired during later sessions. All image interpretations were done blinded to other readers and to the ICA results. The point averages of the 3 readers were used to generate ROC curves using ICA as a gold standard. For the session 3 fusion interpretation, the diagnostician was again shown all the MPI information described above and the ECTb Heartfusion display which shows the superposition of the coronaries from the CTA studies fused onto the 3D myocardial surface modulated by the 3D perfusion distribution. The CTA study was also shown to score session 3 results.

### Statistical Analysis

Continuous data were expressed as mean ± SD. Paired *t* tests were used to compare differences in the continuous data. Discrete variables were expressed as frequency distributions. Two by two table and Chi-square test were used to compare differences in the discrete variables. Normalcy rate was calculated as the number of patients that were interpreted normal or probably normal in the group of patients with <5% LLK of CAD. ROC analysis was used to determine the incremental value of fusion by comparing the readers' interpretation with the three different subsets of images: (1) using MPI alone, (2) using MPI plus CTA, and (3) Using MPI, CTA 3D fused images. A univariate z-score test of the difference between the areas of two ROC curves was used to calculate statistical significance between techniques. Statistical significance was defined as a $P$ value <.05.

# RESULTS

## Baseline Characteristics of Patients

The clinical characteristics of the 50 patients enrolled in this study are presented in Table 1. The 13 low-likelihood subjects had a normal baseline ECG, no induced ECG changes after stress test, no major risk factors for CAD, or a history of previous cardiac events. Patients who underwent ICA (N = 37) had high prevalence of risk factors for CAD. Twenty-one (57%) had arterial hypertension, 29 (78%) had hyperlipidemia, 12 (32%) had diabetes mellitus, and 8 (22%) were current smokers. Fourteen (38%) of 37 patients had undergone previous percutaneous coronary intervention and 15 (40%) had history of myocardial infarction. Twenty-eight of 37 patients (76%) had at least one coronary artery stenosis ≥50% (LAD: 25, LCX: 15, RCA: 16) as observed on ICA and non-critical stenoses were found in 9 of the 37 patients.

## Performance of Image Fusion

In all 50 patients, coronary artery extraction, reconstruction, and fusion were successfully performed. The fused images were automatically generated. Nevertheless, in several patients a manual realignment was necessary to better align the epicardial surface of the myocardial perfusion model with the CTA coronary tree; 6 (12%) patients for the left coronary artery models and 26 (53%) patients for the right coronary artery model. The average time needed for processing and reading the fused images varied from a few minutes to 30 minutes. The extraction of the coronary arteries from the CTAs took the longest time and it was the limiting step. Once the coronary arteries are extracted the fusion took no longer than 1 or 2 minutes (including manual alignment when needed).

## Normalcy Rate

The studies of all 13 patients with LLK of CAD were interpreted as normal or probably normal by the reviewers using MPI alone, MPI + CTA, and Fused MPI/CTA (normalcy rate = 100%).

To determine the confidence of the reviewer's interpretation, the scores by coronary artery territory (LAD, LCX, and RCA) from the three readers were analyzed (Table 2). The confidence of the interpretation was higher with fused images than with MPI alone, and MPI + CTA side-by-side. Nonetheless, the differences were statistically significant only when fusion was compared with MPI alone (Table 2).

## Performance of the Three Methods for the Diagnosis of Obstructive Coronary Artery Disease

Table 3 shows the test characteristics of the three methods for overall CAD and vessel by vessel performance. Image fusion resulted in a non-significant trend for improvement over MPI and MPI-CTA side-by-side. Although these single point statistics were not significant, we obtained significant results when we performed an analysis of area under the receiver operating characteristic curve (AUC) for the three methods (Figure 1). This is probably due to the fact that AUC considers all the points under a curve while sensitivity and specificity provide isolated point comparisons. MPI and CTA read side-by-side showed a trend toward better performance than MPI alone in the overall and individual vessel assessment of CAD (Figure 1). However, these differences were statistically significant only for the LAD territory ($P = .03$). MPI-CTA fusion showed a better performance than MPI and MPI and CTA read side-by-side in the overall assessment of CAD ($P = .005$ vs MPI, $P = .04$ vs MPI + CTA) and the assessment of LAD disease ($P < .001$ vs MPI, and $P = .007$ vs MPI + CTA) (Figure 1).

The following are the areas under the ROC curve (AUC) with 95% confidence intervals in parenthesis for each imaging method. MPI AUC for global CAD: 0.77 (0.60-0.89) LAD: 0.62 (45-77), LCX: 0.66 (0.49-0.81), RCA: 0.85 (0.69-0.94). MPI-CTA side-by-side AUC for global CAD: 0.83 (0.67-0.93), LAD: 0.72 (0.55-0.85), LCX: 0.74 (0.57-0.87), RCA: 0.87 (0.72-0.96). MPI-CTA fusion imagines AUC for global CAD: 0.89 (0.74-0.97), LAD: 0.82 (0.66-0.93), LCX: 0.75 (0.58-0.88), RCA: 0.88 (0.73-0.96). When the CTA information was added to the MPI data, the readers modified their interpretations 50% of the times (Table 4). When the fused images were provided as the last step, the reviewers modified their interpretations 28% of the times compared to the previous step (Table 5). With the addition of fusion imaging we noted a non-significant trend toward improved sensitivity for detection of multi-vessel disease compared to MPI alone and MPI and CTA side-by-side (Figure 2).

The type of MPI study performed (SPECT versus PET) or the model of CT used for CTA (16- versus 64-slice) did not affect the accuracy of interpretation of the fusion studies. The area under the curve for global CAD with the fused images was 0.86 (0.72-0.95) for SPECT vs 0.91 (0.75-0.98) for PET imaging. The area under the curves with the fused images was 0.85 (0.61-0.97) for 16-slice CTA vs 0.90 (0.73-0.99) for 64-slice CTA.

## DISCUSSION

The present study reveals that the fusion of MPI and CTA has incremental diagnostic value over MPI alone and MPI-CTA side-by-side for the detection of obstructive CAD and localization of LAD disease using ICA as the gold standard. The incremental diagnostic value of image fusion was probably due in part to the improved specificity of image fusion, suggesting that fusion shows promise as a tool to help save patients with normal coronaries or non-critical lesions from undergoing cardiac catheterization.

The higher accuracy demonstrated by the fused MPI-CTA methodology for the LAD territory can be partially explained by the smaller amount of manipulation required for the LAD fusion model in comparison with the LCX and RCA fusion model. In fact, in this study user interaction was required in more than 50% of the PDA alignments. Alignment problems frequently affect the PDA and LCX territories, often necessitating user interaction, and sometimes causing misdiagnosis. In this particular series the performance of MPI and CTA for predicting significant disease in the LAD territory was lower than that for the LCX and RCA territories by either method. It should be noted, however, that there was little room for performance improvement with fusion imaging in the RCA territory since the results of MPI alone were very good. Nevertheless, these results indicate a need for further improvement of the automatic alignment of the RCA and LCX coronaries onto the perfusion 3D map, a topic of our ongoing research.

A computer integration of anatomic and physiologic information from CTA and MPI reduces the number of misinterpretations when compared with the mental integration of the two sets of images. This is most likely due to the added diagnostic confidence provided by the 3D alignment of a left-ventricular perfusion defect distal to a vessel stenosis detected on angiography.

Figures 3 and 4, show two examples of improved performance with the fusion technique. The example in Figure 3 shows that computer integration of CTA and MPI helped in the assessment of the physiologic effects of a borderline anatomical lesion. The example in Figure 4 shows that the location of a stenosis with respect to the left ventricular epicardial surface can only be judged approximately, and thus, its physiologic effects may be difficult to determine without the fused images.

Two recent studies addressed the use of MPI and CTA images obtained from separate scanners to investigate the incremental value of image fusion for the diagnosis of CAD. The authors of the first publication used the same fusion approach used in the present study.[10] The second study required manual alignment of the CTA and MPI slices and semi-automated techniques to segment the epicardial boundary from the CTA.[11] The authors then superimposed the volume rendered CT images over the color-coded 3D perfusion map for visual interpretation.[11] In the study by Rispler et al,[10] that included 44 patients, the fusion approach resulted in significant improvement in specificity and positive predictive value and no loss in sensitivity or negative predictive value. The specificity and positive predictive value of fusion imaging as reported in the study by Rispler et al were 95% and 77% compared to 67% and 89% in our investigation.[10] However, it should be noted that Rispler et al excluded from their analyses 12 patients because of poor CTA quality, while our data are based on the results of all 50 patients submitted to imaging.[10] This might have been the cause of the apparent discrepancy in test characteristics. Gaemperli et al focused on the value SPECT/CT fused images to assess the functional relevance of coronary artery stenoses in 38 patients with CAD.[11] They concluded that SPECT/CT fusion images added diagnostic information on the functional relevance of coronary artery stenoses but mainly in branch vessels and every calcified vessels not easily assessable by CTA.

The present study confirms but also extends prior observations. Our results demonstrate the added diagnostic value of fusion of MPI and CTA for predicting critical coronary stenoses when used by nuclear cardiology specialists in a practice setting. In fact, the study was designed to simulate the clinical scenario of a practicing nuclear cardiologist. The initial step was the interpretation of the MPI. Then, the CTA information was added and the readers were allowed to modify their interpretations in view of the newly acquired information (it happened 50% of the times). Finally, the fused images were provided and the reviewers were again allowed to modify their interpretations and this happened 28% of the times. This study also shows that the performance improvement obtained with MPI-CTA fusion is similar when either SPECT or PET imaging modalities or 16-slice or 64-slice CT scanners are used for image acquisition, despite a trend in favor of 64-slice CTA and PET for better performance. Finally, although non-significant, fusion imaging showed a trend toward better sensitivity for detection of multi-vessel disease. Further investigation of this apparent benefit of fusion imaging deserves consideration since it might help solve the dilemma of apparently normal perfusion scans in patients with multi-vessel disease.

There were a few limitations to our study. The number of patients enrolled with obstructive CAD was relatively small. The MPI and CTA studies were performed at different sites and with different techniques. Although the latter can be seen as a weakness, it could also be interpreted as a strength of the study since the performance of MPI and CTA with different techniques and at different sites gave similar results. We detected no performance difference between SPECT and PET, and 16- and 64-slice CTA although a trend toward better results with PET and 64-slice CTA was noted. The absence of a difference in performance of these technologies might have been due to the small sample size. Of course the addition of a CTA to an MPI study implies a substantially higher radiation dose for the patient under analysis. The premise of our work is not that all patients being evaluated for CAD should undergo both MPI and CTA. Rather, that when both studies are performed in a patient, a higher diagnostic accuracy is obtained when interpreting the studies with all available information, including the quantitative information contained in the fused images. It is yet to be established in a large population whether this additional diagnostic accuracy can reduce the additional cost, risk and radiation inherent with cardiac catheterization in a significant number of patients. Finally, the gold standard chosen for the end point of this study (obstructive disease on ICA) does not provide information about the functional significance of the detected lesion. This limitation prevented us from addressing the important issue of

assessing borderline lesions. Moreover, one would expect that ICA tends to agree more with CTA than MPI since both CTA and ICA are anatomical rather than functional tests. Because of this bias we could not and did not perform a head-to-head comparison of CTA and MPI.

In conclusion, our study extends previous reports noting that fusion of MPI and CTA shows incremental diagnostic value over MPI alone, and MPI and CTA read side-by-side for prediction of obstructive CAD on ICA. Future research should investigate the incremental prognostic value of this approach in the appropriate candidate.

## Acknowledgments

This work was funded in part by General Electric healthcare LTD; National Institute of Health, NHLBI grant number K01 HL70422; Carlos III Institute; Thematic networks of cooperative research, (Red C03/01, RECAVA), and National Institute of Health; NHLBI grant number R01 HL085417. Two of the authors (TLF, EVG) receive royalties from the sale of the Emory Cardiac Toolbox™ utilized to conduct the research described in this article. The terms of this arrangement have been reviewed and approved by Emory University in accordance with it is conflict-of-interest practice.

## References

1. Shaw LJ, Shaw RE, Merz CN, et al. Impact of ethnicity and gender differences on angiographic coronary artery disease prevalence and in-hospital mortality in the American College of Cardiology-National Cardiovascular Data Registry. Circulation. 2008; 117:1787–801. [PubMed: 18378615]
2. Schoepf UJ, Becker CR, Ohnesorge BM, Yucel EK. CT of coronary artery disease. Radiology. 2004; 232:18–37. [PubMed: 15220491]
3. Diamond GA, Forrester JS. Analysis of probability as an aid in the clinical diagnosis of coronary-artery disease. N Engl J Med. 1979; 300:1350–8. [PubMed: 440357]
4. Grossman GB, Garcia EV, Bateman TM, et al. Quantitative Tc-99m sestamibi attenuation-corrected SPECT: development and multicenter trial validation of myocardial perfusion stress gender-independent normal database in an obese population. J Nucl Cardiol. 2004; 11:263–72. [PubMed: 15173773]
5. Case JAPT, O'Brian-Penny B, King MA, Luo DS, Rabin MSZ. Reduction of truncation artifacts in fan beam transmission imaging using a spatially varying gamma prior. IEEE-TNS. 1995; 42:1310–20.
6. Nichols KJ, Bacharach SL, Bergmann SR, et al. Instrumentation quality assurance and performance. J Nucl Cardiol. 2006; 13:e25–41. [PubMed: 17174795]
7. Nye JA, Esteves F, Votaw JR. Minimizing artifacts resulting from respiratory and cardiac motion by optimization of the transmission scan in cardiac PET/CT. Med Phys. 2007; 34:1901–6. [PubMed: 17654891]
8. Scanlon PJ, Faxon DP, Audet AM, et al. ACC/AHA guidelines for coronary angiography. A report of the American College of Cardiology/American Heart Association Task Force on practice guidelines (Committee on Coronary Angiography). Developed in collaboration with the Society for Cardiac Angiography and Interventions. J Am Coll Cardiol. 1999; 33:1756–824. [PubMed: 10334456]
9. Faber TL, Santana CA, Garcia EV, et al. Three-dimensional fusion of coronary arteries with myocardial perfusion distributions: Clinical validation. J Nucl Med. 2004; 45:745–53. [PubMed: 15136621]
10. Rispler S, Keidar Z, Ghersin E, et al. Integrated single-photon emission computed tomography and computed tomography coronary angiography for the assessment of hemodynamically significant coronary artery lesions. J Am Coll Cardiol. 2007; 49:1059–67. [PubMed: 17349885]
11. Gaemperli O, Schepis T, Valenta I, et al. Cardiac image fusion from stand-alone SPECT and CT: Clinical experience. J Nucl Med. 2007; 48:696–703. [PubMed: 17475956]

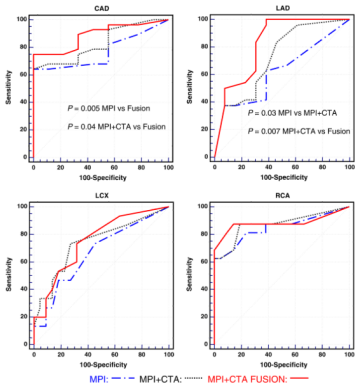


**Figure 1.**

Detection and localization of coronary artery disease using myocardial perfusion imaging alone, myocardial perfusion imaging and computed tomography angiography side-by-side, and fusion of myocardial perfusion imaging and computed tomography angiography. Significant disease is defined as ≥50% luminal coronary stenosis by invasive coronary angiography. *CAD*, Coronary artery disease; *CTA*, computed tomography angiography; *LAD*, left anterior descending coronary artery; *LCX*, left circumflex coronary artery; *MPI*, myocardial perfusion imaging; *RCA*, right coronary artery.

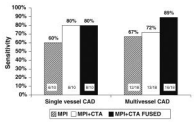


**Figure 2.**

Sensitivity for identification of single vessel and multi-vessel vessel coronary artery disease (CAD) of myocardial perfusion imaging alone (MPI), myocardial perfusion imaging and computed tomography angiography side-by-side (MPI + CTA), and fusion imaging (MPI + CTA FUSED).

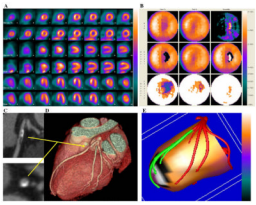

**Figure 3.**

Example of fusion imaging in a patient with single vessel coronary artery disease. **A**, Short axis, vertical and horizontal long axis slices of the Stress/Rest SPECT study. This perfusion study was read as probably normal. **B**, Polar maps of the same SPECT study. **C**, Multi-planar reconstructions of the coronary arteries on CT angiography showing a plaque in the proximal left anterior descending coronary artery. This was read as equivocal for coronary artery disease. **D**, Three-dimensional rendering of the coronary arteries on CT angiography showing the paths of the coronary arteries and the plaque location in the left anterior descending coronary artery. **E**, Fused display; the black area on the fused display identifies a region of myocardial hypoperfusion during stress. The white area within the black region indicates an area of reversibility of the perfusion abnormality. The segments of the coronary arteries rendered in green are segments distal to stenoses seen on CT angiography. This fused scan was read as showing obstructive coronary artery disease in the left anterior descending coronary artery territory. Since the invasive angiogram results showed a 50% proximal left anterior descending coronary artery lesion, only the fused display was interpreted accurately.

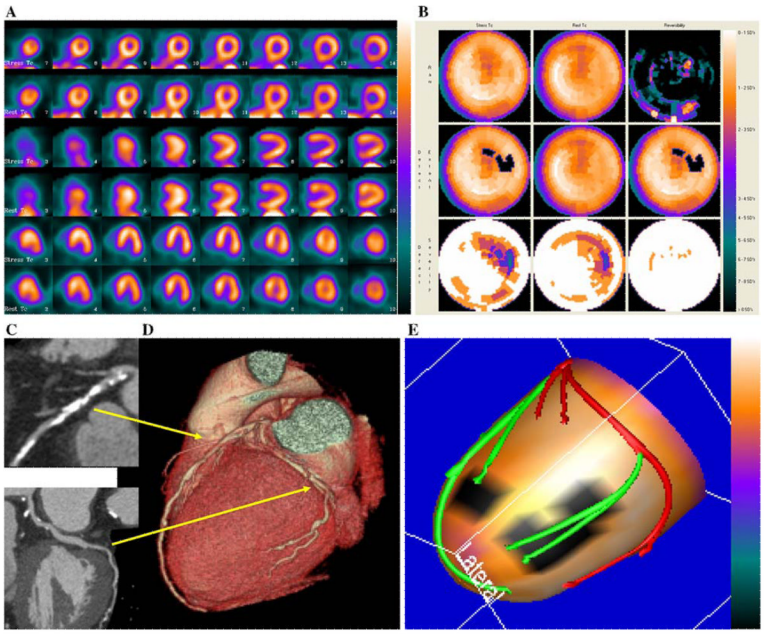


**Figure 4.**

Example of fusion imaging in a patient with multi-vessel coronary artery disease. **A**, Short axis, vertical and horizontal long axis slices of the stress/rest SPECT. It was read as probably normal. **B**, Polar maps of the same SPECT study. **C**, Multi-planar reconstructions of the coronary arteries on CT angiography showing a plaque in the proximal left anterior descending coronary artery and possible stenosis in the left circumflex coronary artery. **D**, Three-dimensional rendering of the coronary arteries on CT angiography showing the paths of the coronary arteries and location of plaques seen in the multi-planar reformations in 3B. **E**, Fused display; the black area on the fused display identifies a region of myocardial hypoperfusion during stress. The segments of the coronary arteries rendered in green are segments distal to stenoses seen on CT angiography. This fused display was read as positive for coronary artery disease. Invasive angiography showed a 50% proximal left anterior descending coronary artery stenosis and a 90% stenosis in the first marginal vessel; thus the fused display was interpreted correctly.

## Table 1

Clinical and demographic characteristics of 50 enrolled subjects

| | **Patients with suspected coronary artery disease N = 37** | **Low-likelihood patients N = 13** |
|---|---|---|
| Mean age | 58 ± 10 | 48 ± 10 |
| Men | 25 (68%) | 9 (69%) |
| Race | | |
| Black | 6 | 2 |
| White | 29 | 7 |
| Hispanic | 1 | 2 |
| Asian | 1 | 1 |
| Unknown | 0 | 1 |
| Hypertension | 21 (57%) | 3 (23%) |
| Diabetes mellitus | 12 (32%) | 0 |
| Hyperlipidemia | 29 (78%) | 5 (38%) |
| Smoking | 8 (22%) | 1 (8%) |
| Prior myocardial infarction | 15 (40%) | 0 |
| Prior revascularization | 14 (38%) | 0 |

## Table 2

Results of readers' interpretation by major coronary artery in patients with low likelihood of CAD (39 interpretations: 13 patients × 3 coronary artery territories)

| | Normal | Probably normal |
|---|---|---|
| MPI alone | 33 (85%) | 6 (15%) |
| MPI + CTA | 38 (97%) | 1 (3%) |
| Fused MPI/CTA | 39 (100%)* | 0 |

* $P = .03$ vs MPI alone.

*CTA*, Computed tomography angiography; *MPI*, myocardial perfusion imaging.

**Table 3**

Test characteristics of the three methods used to diagnose obstructive coronary artery disease in the 37 patients submitted to invasive angiography; none of the comparisons was statistically significant. The confidence intervals are shown in parentheses

| | Overall coronary artery disease | | | Vessel specific analysis | | |
|---|---|---|---|---|---|---|
| | **MPI** | **MPI + CTA** | **Fused** | **MPI** | **MPI + CTA** | **Fused** |
| Sensitivity | 82% (63–93) | 79% (59–92) | 89% (72–98) | 65% (52–78) | 75% (61–85) | 76% (63–87) |
| Specificity | 44% (14–79) | 56% (21–86) | 67% (30–92) | 71% (58–83) | 77% (64–87) | 80% (68–90) |
| Accuracy | 73% (56–86) | 73% (56–86) | 84% (68–94) | 68% (59–77) | 76% (67–83) | 78% (70–86) |

*CTA*, Computed tomography angiography; *MPI*, myocardial perfusion imaging.

## Table 4

Change in diagnostic impression in each patient category due to the addition of computed tomography angiography to myocardial perfusion imaging

| | Obstructive coronary artery disease | Non-obstructive coronary artery disease | Low likelihood of coronary artery disease | Total |
|---|---|---|---|---|
| Less disease | 2 (7%) | 5 (56%) | 4 (31%) | 11 |
| More disease | 10 (36%) | 3 (33%) | 1 (7%) | 14 |
| No changes | 16 (57%) | 1 (11%) | 8 (62%) | 25 |
| Total | 28 | 9 | 13 | 50 |

## Table 5

Change in diagnostic impression in each patient category due to the addition of fused images to computed tomography angiography and myocardial perfusion imaging

| | Obstructive coronary artery disease | Non-obstructive coronary artery disease | Low likelihood of coronary artery disease | Total |
|---|---|---|---|---|
| Less disease | 1 (4%) | 4 (45%) | 1 (8%) | 6 |
| More disease | 6 (21%) | 2 (22%) | 0 | 8 |
| No changes | 21 (75%) | 3 (33%) | 12 (92%) | 36 |
| Total | 28 | 9 | 13 | 50 |